Journal of Magnetism and Magnetic Materials 501 (2020) 166431

Contents lists available at ScienceDirect

Journal of Magnetism and Magnetic Materials

journal homepage: www.elsevier.com/locate/jmmm

Research articles

Correlating magnetic properties of ferritic NO electrical steel containing 2.4 m.%Si with hot strip microstructure

A. Stoecker[a,*], N. Leuning[b], K. Hameyer[b], X. Wei[c], G. Hirt[c], S. Korte-Kerzel[d], U. Prahl[a], R. Kawalla[a]

[a] Institute of Metal Forming, TU Bergakademie Freiberg, 09596 Freiberg, Germany
[b] Institute of Electrical Machines, RWTH Aachen University, 52062 Aachen, Germany
[c] Institute of Metal Forming, RWTH Aachen University, 52056 Aachen, Germany
[d] Institute of Physical Metallurgy and Metal Physics, RWTH Aachen University, 52074 Aachen, Germany

ARTICLE INFO

Keywords:
Hot rolling
Non-oriented electrical steel
Grain size
Texture
Magnetization

ABSTRACT

Understanding the interdependencies of the processing steps of high silicon containing non-oriented (NO) electrical steel is a key factor for improving its final magnetic properties. Moreover, every process step in the production has a significant impact on the properties. Steels with a high silicon content are ferritic (α-Fe). Accordingly, the microstructure and texture are inherited from one processing step to the next. The presented research relates the hot strip microstructure and texture to the magnetic properties of the final annealed material. To investigate the impact of hot strip microstructure and texture for a ferritic 2.4 m.%Si silicon containing steel, the material was hot rolled from an initial thickness of 64 mm down to a thickness of 1 mm whereby different microstructures and textures were achieved by varied hot rolling conditions. Subsequently, the material was cold rolled to 0.25 mm and annealed at 800 °C or 1000 °C for 3 min. Finally, samples of each processing step were analyzed by means of light microscopy and XRD texture measurements. Samples after hot rolling and final annealing were tested in a single sheet tester for specific losses and magnetic polarization. Findings show an influence of the initial hot strip microstructure on the microstructure and magnetic properties of the final annealed samples.

1. Introduction

In a rotation machine, the angle between the magnetic field and the lamination direction changes continuously due to the rotating magnetic field. Consequently, the lamination material made of non-oriented (NO) electrical steel should provide isotropic magnetic behavior and good magnetic properties, for example a high magnetization and low losses. These magnetic properties depend closely on the grain size and crystallographic texture of the material. For this reason, a beneficial grain size and texture in the fully processed material is needed. Considering grain size, a specific grain size for each application is required. On the other hand, the θ-texture-fiber [1] seems adequate, where ⟨001⟩ directions are parallel to normal direction (ND), for example rotated cube {1 0 0}⟨1 1 0⟩ as ideal orientations, and thereby, directions of easy magnetization are in the sheet plane. In addition, the Goss texture {1 1 0}⟨0 0 1⟩ is beneficial as well [2].

To improve the magnetic properties in the final product, an optimization of the production prior to final annealing is necessary. Especially for ferritic NO grades the interdependencies along the processing steps need to be considered [3–6]. One approach is to control the hot strip microstructure and texture to observe favorable interactions with the following processing steps. Certain researches state that a large ferrite grain size prior to cold rolling is an important factor for the magnetic performance of high silicon non-oriented electrical steel grades [7–10]. However, it is necessary to distinguish between the influence of hot strip grain size and hot strip texture. The texture after cold rolling seems to be independent on initial hot strip grain size [11]. In contrast, the hot strip grain size has a large impact on size and shape of the deformed grains after cold rolling [11].

For further investigations of the dependency of magnetic properties on hot strip microstructure and texture, three hot strips with different grain size and texture were cold rolled and annealed. Finally, the magnetic properties, particularly magnetization and losses, were measured and evaluated with respect to the hot strip microstructure.

* Corresponding author.
E-mail address: anett.stoecker@imf.tu-freiberg.de (A. Stoecker).

https://doi.org/10.1016/j.jmmm.2020.166431
Received 31 August 2019; Received in revised form 16 December 2019; Accepted 9 January 2020
Available online 11 January 2020

2. Experimental procedure

In this study, a typical ferritic NO electrical steel alloy containing 2.4 m.%Si Si and 0.3 m.%Si Al was used. A continuous cast thin slab with a thickness of 64 mm was used as feedstock which shows a columnar grain structure and an average grain size over 1000 µm. After reheating the thin slab and soaking for 60 min at 1200 °C, the material was hot rolled in 9 passes to a final hot strip thickness of 1 mm using a four-stand semi-continuous hot rolling mill. The hot rolling start temperature was 1180 °C, and a finishing temperature of 890 °C was achieved. After the last pass of hot rolling, sample A was water quenched to freeze the microstructure. Sample B experienced air cooling, sample C was directly moved in an air circulation furnace with a furnace temperature of 800 °C and cooled to room temperature with 50K/h.

For evaluating the impact of the hot strip microstructure, all three samples were identically cold rolled within 7 passes to 0.25 mm on a laboratory rolling mill. Finally, the samples were annealed for three minutes at annealing temperatures ϑ_a of 800 °C or 1000 °C. By these temperatures and annealing duration, a fully recrystallized grain morphology is guaranteed.

Light microscopy images were taken in the normal direction (ND) – rolling direction (RD)-plane after hot rolling, cold rolling, and final annealing (Fig. 1, 3, and 5). To express the grain size, the mean lineal intercept method in the ND-RD-plane parallel RD was used with a total of 300 grains of each inspected layer of the samples. The results in terms of mean lineal intercept length are listed in Table 1.

Since microstructure and texture are heterogeneous through the strip thickness, texture was measured in three through-thickness layers in the transversal direction (TD)-RD-plane of the sheet. The parameter s describes the inspected layer. This parameter is defined as $s = 2a/d$ with a being the distance of the actual layer from the center layer and d the sample thickness. To determine crystallographic macro texture of all samples, incomplete pole figures were measured with X-ray diffraction by a Bruker D8 Advanced diffractometer, equipped with a High Star area detector and orientation distribution functions (ODF) were calculated using the Matlab®toolbox MTEX version 4.5.1 [12]. All relevant orientations and fibers for NO electrical steels are within the $\varphi_2 = 45°$ section of the Euler space, therefore this section is chosen for texture representation.

In order to identify the dependence of the magnetic properties of the fully processed material on hot strip microstructure and texture, magnetic measurements are performed on a 60 mm × 60 mm Single-Sheet-Tester with Brockhaus measurement equipment. *J-H*-hysteresis curves at polarizations between 0.1 T and 1.8 T at different frequencies of 50 HZ and 400 HZ are analyzed under sinusoidal magnetic flux excitation. For all hot strips and final annealed samples, square parts along RD and TD direction were cut by guillotine shears and afterward magnetically characterized. The sample geometry assures that there is no influence from the cutting process. In order to ensure comparability of the measurements, the form factor is used as a quality criterion for the sinusoidal excitation and measurement results. The allowed form factor error is less than 1%.

Table 1
Mean lineal intercept length in µm for hot strip and after annealing at 800 °C or 1000 °C, values based on 300 measured grains by lineal intercept method parallel to RD.

Material	State	s = 0.9	s = 0.5	s = 0	Average
A	Hot strip	–	–	-	–
	ϑ_a = 800 °C	8.2	8.4	11.9	8.7
	ϑ_a = 1000 °C		*Not subdivided*		55.7
B	Hot strip	14.2	–	–	–
	ϑ_a = 800 °C	6.6	8.4	12.0	9.1
	ϑ_a = 1000 °C		*Not subdivided*		54.7
C	Hot strip	30.8	44.7	57.8	44.7
	ϑ_a = 800 °C	14.7	16.6	21.4	17.7
	ϑ_a = 1000 °C		*Not subdivided*		68.0

3. Results and discussion

3.1. Characterization of microstructure and texture of the hot strip

Dependent on the hot rolling conditions, a heterogeneous microstructure was produced, see Fig. 1. Differences appear between surface near areas and hot strip center. For water cooling after the last pass of hot rolling (hot strip A, Fig. 1(a)), non-terminating bands are present in the strip center over two third of the cross section. However, the near surface area consists of elongated deformed grains. Due to this grain morphology, grain size measurement was not performed. In contrast, a slow cooling with 50K/h after finish rolling results in a fully recrystallized equiaxed grain shape across the complete thickness of the hot strip (Fig. 1(c)). Differences between surface and center area in grain size exist, see Table 1. Overall, hot strip C has a mean intercept length of 45 µm, with twice the grain size in the center than at the surface.

Based on the processing conditions of the hot strips, hot strip C is the result of an annealing process of hot strip A. This assumption is based on the idea to consider slow cooling from 800 °C to room temperature with 50 K/h as a kind of hot strip annealing.

The micrograph of hot strip B (Fig. 1(b)) reveals an intermediate state of the previous described conditions. Besides the small recrystallized grains near the surface with a mean intercept length of 14 µm, a band structure with wavy grain boundaries, indicating recovery, characterizes this hot strip.

Correlating with the grain morphology, different textures are found. Fig. 2 gives an overview of the hot strip texture at the sample surface $s = 0.9$ and the sample center $s = 0$. Generally, a typical hot rolled texture for body centered cubic iron silicon steel with a strong texture gradient between surface and center is observed [1]. Near surface areas show a pronounced Goss texture due to shear during the hot rolling process. In contrast, in the center plane strain deformation is dominant

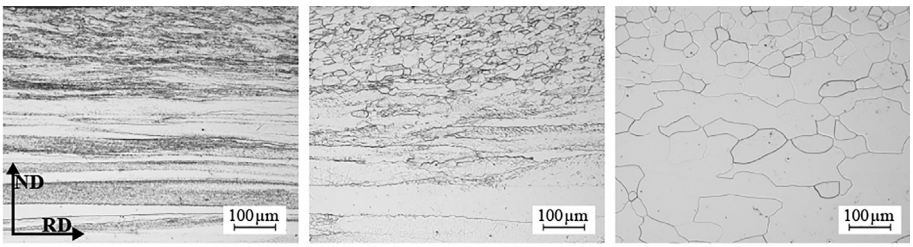

(a) hot strip A (b) hot strip B (c) hot strip C

Fig. 1. Micrographs of studied hot strips, top of pictures represents surface areas and bottom of pictures strip center.

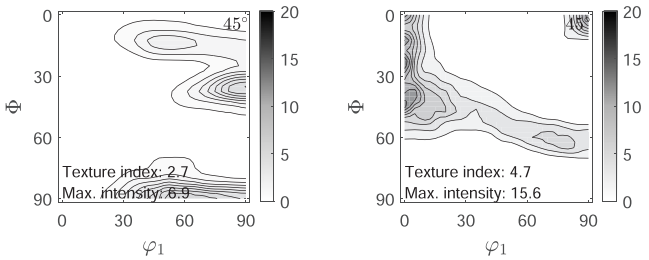

(a) hot strip A, $s = 0.9$ (b) hot strip A, $s = 0$

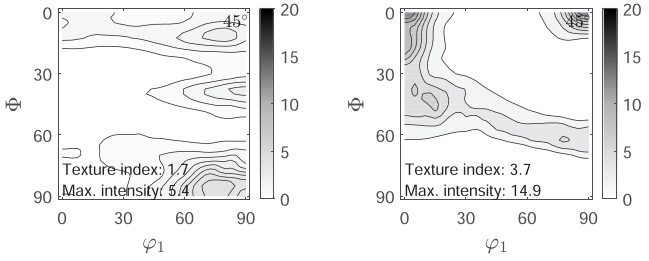

(c) hot strip B, $s = 0.9$ (d) hot strip B, $s = 0$

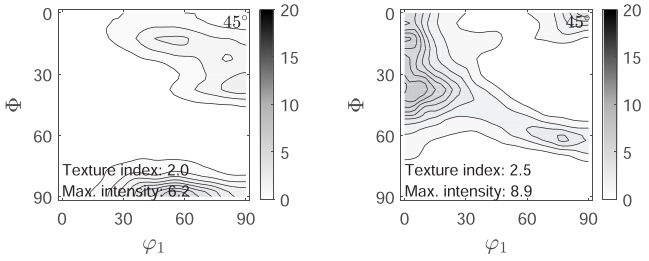

(e) hot strip C, $s = 0.9$ (f) hot strip C, $s = 0$

Fig. 2. $\varphi_2 = 45^\circ$ section of the Euler space in Bunge notation for strip surface $s = 0.9$ and strip center $s = 0$ of the investigated hot strips.

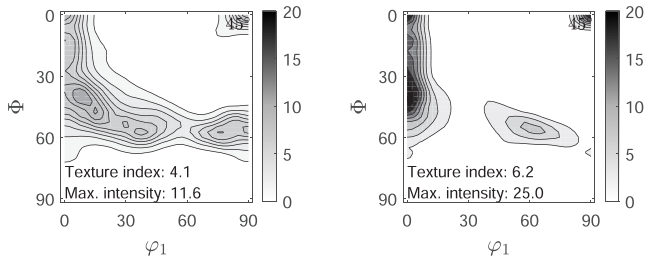

(a) cold strip A, $s = 0.9$ (b) cold strip A, $s = 0$

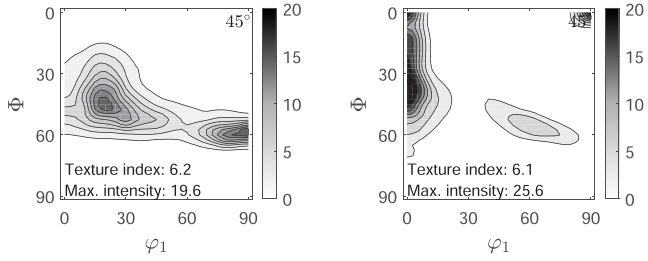

(c) cold strip B, $s = 0.9$ (d) cold strip B, $s = 0$

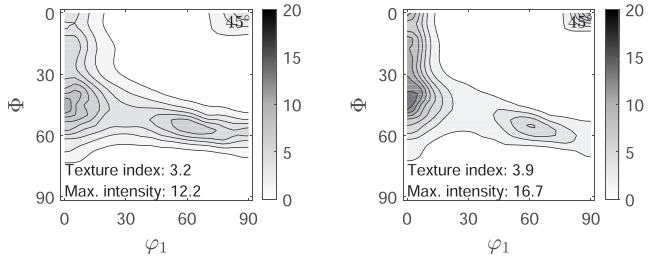

(e) cold strip C, $s = 0.9$ (f) cold strip C, $s = 0$

Fig. 4. $\varphi_2 = 45^\circ$ section of the Euler space in Bunge notation for strip surface $s = 0.9$ and strip center $s = 0$ of cold rolled material.

leading to a strong α-fiber and a weak γ-fiber. Nevertheless, the textures show dissimilar maximum orientations. As described above, hot strip A has a deformed structure which is accompanied with stronger α-fibre in contrast to hot strip B and C. Also, hot strip B has a maximum at rotated cube, $(0\,0\,1)[1\,1\,0]$, in the α-fiber, which was preserved by recovery.

3.2. Characterization of microstructure and texture after cold rolling and final annealing

Fig. 3 shows the micrographs after cold rolling. The grains are elongated in the rolling direction. Due to the initially recrystallized large grains in hot strip C, the grains are still visible after the high reduction in cold rolling. No shear bands are present spanning the sheet thickness. However, localized planar deformation is observed within individual grains, indicated by arrows in Fig. 3(c).

Fig. 4 shows the texture after cold rolling. Compared with the hot strips, the cold strips show sharper texture, i.e. the orientations are more concentrated. This shows that several preferential orientations can be induced by cold rolling, namely rotated cube, $(1\,1\,2)[1\,\bar{1}\,0]$ in α-fiber and $(1\,1\,1)[0\,\bar{1}\,1]$ in γ-fiber. Because of the different texture in the hot strips, the three preferential orientations are retained and/or generated at different levels. However, the texture of cold strips A, B and C are similar after cold rolling.

After final annealing, the grain morphology reveals a fully

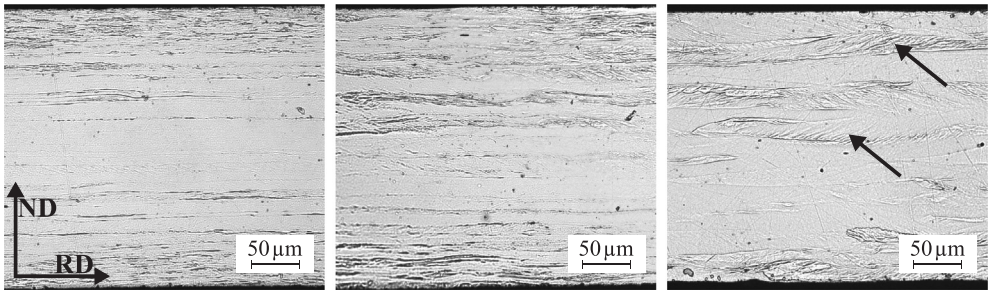

(a) cold strip A (b) cold strip B (c) cold strip C

Fig. 3. Micrographs of investigated cold strips, thickness 0.25 mm, arrows in (c) indicate localized planar deformation in individual grains.

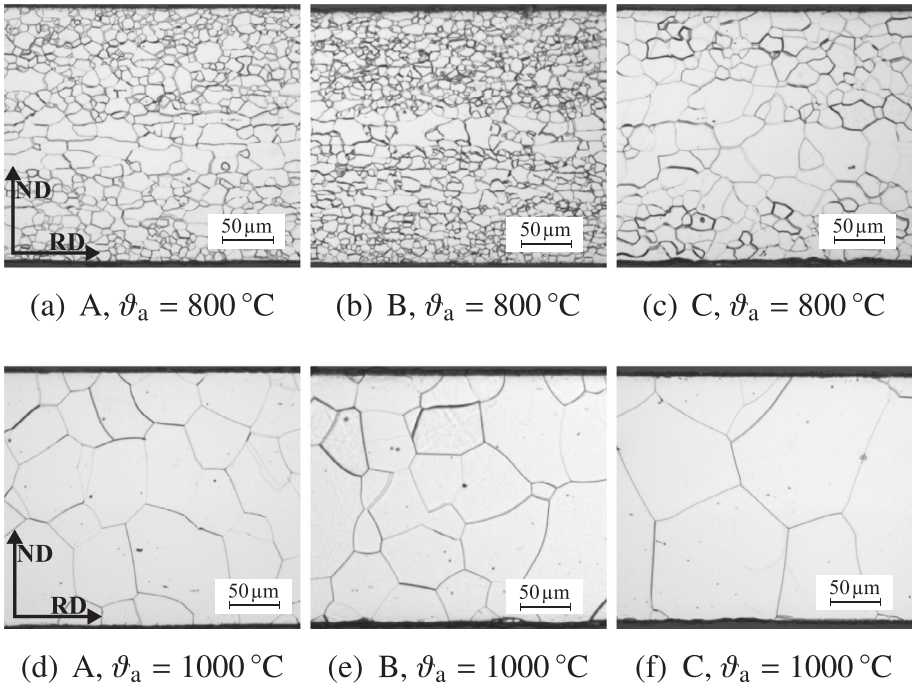

Fig. 5. Micrographs of investigated samples after final annealing at 800 °C and 1000 °C.

recrystallized material with mean lineal intercept length between 9 µm and 68 µm (detailed results are presented in Fig. 5 and Table 1). As expected, larger grains could be found in the 1000 °C annealed samples where grain growth already took place. This leads also to a homogeneous grain size across the sheet thickness while at 800 °C the grains first become bigger at the sheet center. The results show that the slow cooling after the hot rolling (material C) will result in a larger grain size after final annealing, whereas material A and B show no significant difference.

Besides the final grain size, texture is an important parameter which directly influences the magnetic properties of NO electrical steels. After recrystallization, the differences across the sheet thickness are nullified, see Fig. 6. Independent of the temperature a decrease in α-fiber components can be observed while the γ-fiber has nearly the same volume fraction. A decrease in α- and γ-components is favored because of their disadvantageous influence on the magnetic properties. Besides that, the favored rotated cube orientation {1 0 0}⟨1 1 0⟩ is eliminated during the grain growth at 1000 °C.

3.3. Magnetic properties of hot strip and final annealed sheets

The three initial hot strips A, B and C are metrologically characterized on a SST in the hot strip state and after final annealing. Due to the fact that final thickness as well as the alloying is identical for all of the annealed samples, the differences in the magnetic behavior can be attributed to the changes in microstructure and texture. The grain size is expected to dominantly affect the magnetic loss, whereas the magnetization behavior is expected to be affected by texture and grain size, depending on the polarization level [6,13,14].

In Fig. 7, the magnetization curves (a) and magnetic loss (b) for the annealed samples are displayed for a frequency of 50Hz. For the magnetic loss P_s, the expected relation between annealing temperature, grain size and magnetic loss can be observed. As expected, annealing at 800 °C leads to smaller grains and thus, higher loss for this frequency. The magnetic loss can be separated into three different components (1), based on [2,15],

$$P_s = P_{hyst} + P_{cl} + P_{exc}. \quad (1)$$

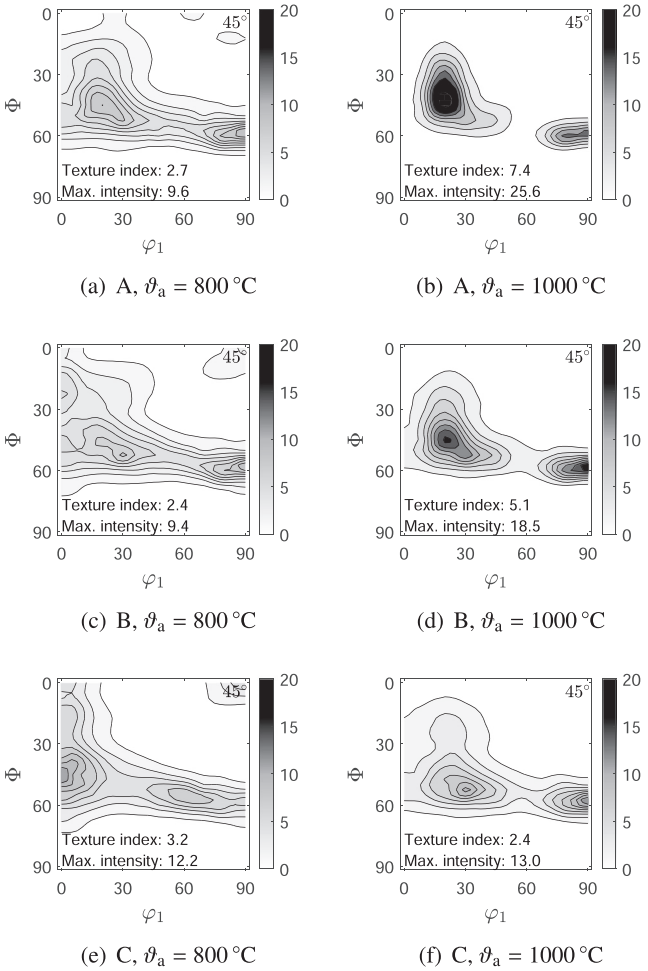

Fig. 6. φ_2 = 45° section of the Euler space in Bunge notation after final annealing at 800 °C and 1000 °C, texture measurements are averaged according to $ODF = 0.25 \cdot ODF_{s0.9} + 0.50 \cdot ODF_{s0.5} + 0.25 \cdot ODF_{s0}$.

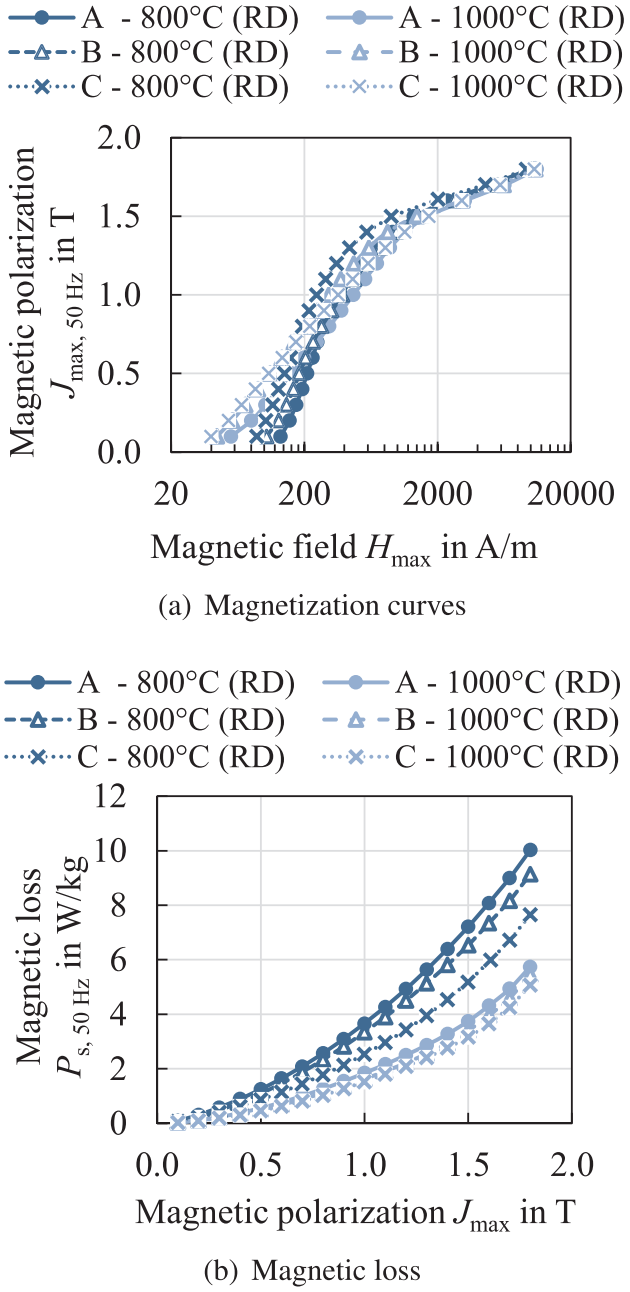

Fig. 7. Magnetic properties of final annealed material at 50 Hz in rolling direction (a) magnetic loss, (b) magnetization curves.

According to [16,17] the hysteresis loss component P_{hyst} decreases with increasing grain size, whereas classical eddy current loss P_{cl} is independent of microstructural features. The third main component, the excess loss P_{exc} increases with increasing grain size [18–20]. Consequently, an optimum grain size can be defined that ensures lowest loss [17]. However, due to the different frequency behavior of the loss components, this minimum depends on frequency. For low and medium frequencies, where hysteresis loss is distinctly more dominant than the excess loss, coarser grain structure leads to smaller loss, as observed in [4]. Additionally, an impact of the hot strip can be observed. For both annealing temperatures, material A exhibits the highest loss, whereas material B has slightly lower losses over the entire polarization range and for both annealing temperatures, material C has the smallest overall loss with the highest grain size. The grain size for A and B is almost the same. The differences between A, B and C are more pronounced for the lower annealing temperature compared with the high annealing temperature.

The magnetization behavior, as depicted in Fig. 7 (a), is more complex. A noticeable difference for the two annealing temperatures can be found in the shape of the magnetization curves. The curves for the samples annealed at 800 °C have a steeper slope at the beginning, i.e. at low polarizations and a higher knee point. The higher annealed samples have a more linear magnetization curve. These differences in shape, result in various crossings of the magnetization curves. At low polarization where domain wall movement is dominant according to [13,14], larger grain sizes lead to easier magnetization. At higher polarizations, the texture is expected to affect the magnetization curve. Because the texture is not quantified in a value, a direct correlation cannot be obtained for the studied materials. In saturation, all curves are congruent, because of the same alloying. Although the results are presented for samples measured in rolling direction, samples in transverse direction are tested as well. The general tendencies are also analogous, so that the presented results for RD can be directly transferred to the transverse direction.

The magnetic properties of the hot strip bear no direct relevance for the application of NO electrical steel, because the hot strip is cold rolled and annealed before it is cut and stacked to build the magnetic core of electrical machines. However, if the assumption, that the magnetic properties are a product of the direct influences and interactions of material characteristics, e.g., alloying, microstructure, texture, sheet thickness or homogeneity, is correct, the relations should consequently apply to the hot strip material as well. In Fig. 8(a), the hot strip material behavior is displayed alongside the final annealed samples for the magnetic loss at 1.0 T and 50 Hz. The hot strips quantitatively have the highest loss. A distinct difference between the three hot strips A, B and C is evident, as it was for the annealed samples. In order to evaluate the effect of grain size from the graph, the effect of sheet thickness has to be accounted for, because sheet thickness d_{sheet} contributes to the classical

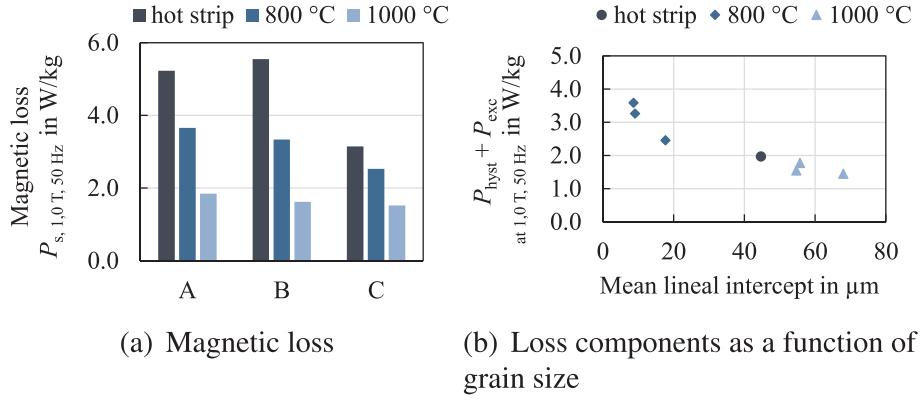

Fig. 8. Magnetic properties of hot strip and final annealed material at 50 Hz and 1.0 T.

Table 2
Magnetic loss components at 1.0 T and 50 Hz determined by (2) and (3) for sample C.

	d_{sheet} in mm	P_s in W/kg	P_{cl} in W/kg	$P_{hyst} + P_{exc}$ in W/kg
C – hot strip	1.00	3.14	1.31	1.83
C – ϑ_a = 800 °C	0.25	2.53	0.074	2.45
C – ϑ_a = 1000 °C	0.25	1.52	0.074	1.44

eddy-current loss component. The hot strip thickness is four times the thickness of the cold-rolled and annealed samples.

The classical eddy-current loss component can be calculated solely from physical parameters as displayed in Eq. (2) in the case of sinusoidal excitation, where, $\hat{B}$ is the peak induction, d_{sheet} the sheet thickness, f the frequency, ρ the material density, and ρ_{el} electrical resistivity.

$$P_{cl} = \frac{(\pi \cdot \hat{B} \cdot f \cdot d_{sheet})^2}{6 \cdot \rho \cdot \rho_{el}} \tag{2}$$

With a ρ_{el} of 0.455μΩm for the material, the hot strip of 1.0 mm thickness has a P_{cl} at 50 Hz a 1.0 T of approximately $1.18\frac{W}{kg}$, whereas for a 0.25 mm strip P_{cl} is below $0.1\frac{W}{kg}$. The results for C are exemplary displayed in Table 2. If the contribution due to thickness is subtracted from the total loss P_s, only the hystersis and excess loss component remain following,

$$P_s - P_{cl} = P_{hyst} + P_{exc}. \tag{3}$$

The results with the approach of (3), as displayed in Fig. 8 (b), display the expected trend of decreasing low frequency loss with increasing grain size, while including the hot strip material state. These are valuable results, as they identify the grain size as dominant for magnetic loss compared to the texture influence. The hot strip texture has more favorable components for the magnetic properties, but the results show a distinct trend only to grain size. In order to distinguish the effect of texture on losses a set of samples with the same grain size and different textures would be needed for future experiments.

3.4. Through process microstructure and texture evolution and influence on magnetic properties

After cold rolling, the initial heterogeneous hot strip microstructure was inherited. The coarse hot strip grains of sample C were the reason for elongated grains after cold rolling, with localized planar deformation in single grains. However, after cold rolling the hot strip with a deformed microstructure (sample A) and partly recrystallized microstructure (sample B), the elongated bands in the strip center were preserved and the sub-surface areas were elongated, as well. The three different hot strips are leading to a different amount of strain hardening after cold rolling. Assuming that these deformed morphology indicates areas with high stored energy, these volumes are consisting of a high density of nucleus for recrystallization. Consequently, a smaller grain size after annealing should be generated in contrast to a volume with lower nucleus density. Indeed, for annealing at 800 °C, where grain growth was not as dominant as at the annealing temperature of 1000 °C, the sub-surface has a smaller grain size in contrast to the center, see Table 1. Whereby, sample C has already at ϑ_a = 800 °C an overall larger grain size, which is beneficial for magnetization and magnetic losses.

Considering texture evolution along the process steps, it is evident that the previous process step influences the texture of the following. After cold rolling, the typical cold rolling texture components of α-fiber and γ-fiber are present with different configurations depending on the initial hot strip texture. The dominant Goss-texture at the near surface layer of the hot strip changes to γ-fiber after cold rolling. This behavior is similar for all investigated materials. At the strip center the α-fiber and γ-fiber of sample C becomes stronger after cold rolling. Whereas, in sample A and B the rotated cube component was preserved and the α-fiber became more dominant. These results are in good accordance with cold rolling texture simulation results [5] and investigations of ferritic rolling texture development in low- and extra low carbon steels [21].

After final annealing, the differences of texture across the sheet thickness were reduced. Therefore, texture was averaged according to $ODF = 0.25 \cdot ODF_{s0.9} + 0.50 \cdot ODF_{s0.5} + 0.25 \cdot ODF_{s0}$, see Fig. 6. The γ-fiber texture with a similar intensity is present after final annealing at 800 °C for all three samples. Despite that, the magnetic properties are unequal. Samples A and B show a very similar behavior. In contrast, sample C has lower magnetic loss and is easier to magnetize for all measured magnetic polarizations. These difference are accountable due to the difference in grain size.

To achieve large grains, high annealing temperatures are required. At those temperatures, favored orientated grains are more likely to disappear. Like Fig. 6 (d) to (f) depicts, the magnetic favorable rotated cube texture vanished. Nevertheless, magnetic losses decreased for the higher annealing temperature. The magnetization curves are more complex. Depending on the polarization, each material has the easiest magnetization at some point.

The characterization of the magnetic properties highlight the impact of hot strip state on the magnetic properties achieved after final annealing. Dependent on hot strip homogeneity the magnetic properties are affected even though all other processing steps apart from hot strip cooling are performed identically. Especially beneficial hot strip microstructures need to be identified and their subsequent processing adapted, in order to improve the final application of non-oriented electrical steels.

4. Conclusion

In the present work, the impact on magnetic properties of three in grain size and texture different 1 mm thick hot strips were investigated. The following processing steps of cold rolling (total reduction 75%) and final annealing (800 °C and 1000 °C) were identical. The results of the investigations of the influence of hot rolling finishing conditions on the magnetic properties of a non-oriented electrical steel with 2.4m.%Si silicon lead to the following conclusions:

- The hot strip microstructure and texture influences the magnetic properties of a fully processed material by its impact on cold rolling morphology and texture, as well as texture and grain size forming during final annealing.
- A large hot strip grain size of average 45 μm (sample C) leads to the lowest overall magnetic losses at 50Hz. Due to the largest hot strip grain size of the investigated hot strip states, after annealing the grains were also larger in comparison to the deformed initial hot strip or partly recrystallized initial hot strip. By magnetic measurements on the fully processed material, the dependencies of the different factors were determined.
- Based on the assumption that the magnetic properties are a product of the material characteristics, e.g., alloying, microstructure, texture and sheet thickness, the same general relations between microstructure, texture and magnetic properties should be valid for the hot strip state. The magnetic measurements of the hot strip show that the basic relation between grain size and magnetic losses can be transferred to the hot strip.
- The processing of the hot strips differed only in the cooling conditions after the last pass of hot rolling. Given that the cooling condition after hot rolling is only one of several hot rolling parameters, improving the magnetic properties by specific hot rolling conditions has a high potential.

Declaration of Competing Interest

The authors declare that they have no known competing financial interests or personal relationships that could have appeared to influence the work reported in this paper.

Acknowledgment

The work of the authors is funded by the Deutsche Forschungsgemeinschaft (DFG, German Research Foundation) – 255681924, 255707264, 255711070, 255713208; and was performed in the research unit 1897 “Low-Loss Electrical Steel for Energy-Efficient Electrical Drives”. Special thanks to S. Roggenbuck for texture measurements.

References

[1] D. Raabe, Steel Res. 74 (2003) 327–337, https://doi.org/10.1002/srin.200300194.
[2] A.J. Moses, Scr. Mater. 67 (2012) 560–565, https://doi.org/10.1016/j.scriptamat.2012.02.027.
[3] S. Steentjes, N. Leuning, J. Dierdorf, X. Wei, G. Hirt, H. Weiss, W. Volk, S. Roggenbuck, S. Korte-Kerzel, A. Stoecker, R. Kawalla, K. Hameyer, IEEE Trans. Magn. 52 (2016) 2001504, https://doi.org/10.1109/TMAG.2016.2516340.
[4] N. Leuning, S. Steentjes, A. Stöcker, R. Kawalla, X. Wei, J. Dierdorf, G. Hirt, S. Roggenbuck, S. Korte-Kerzel, H.A. Weiss, W. Volk, K. Hameyer, AIP Adv. 8 (2018) 047601, , https://doi.org/10.1063/1.4994143.
[5] R. Kawalla, A. Stöcker, U. Prahl, X. Wei, J. Dierdorf, G. Hirt, M. Heller, S. Roggenbuck, S. Korte-Kerzel, H.A. Weiss, P. Tröber, L. Böhm, W. Volk, N. Leuning, K. Hameyer, AIMS Mater. Sci. 5 (2018) 1184–1198, https://doi.org/10.3934/matersci.2018.6.1184.
[6] N. Leuning, S. Steentjes, K. Hameyer, J. Magn. Magn. Mater. 469 (2019) 373–382, https://doi.org/10.1016/j.jmmm.2018.07.073.
[7] S. Paolinelli, M. Cunha, S. Daf, A. Cota, IEEE Trans. Magn. 48 (2012) 1401–1404.
[8] J.-T. Park, J.A. Szpunar, J. Magn. Magn. Mater. 321 (2009) 1928–1932, https://doi.org/10.1016/j.jmmm.2008.12.015.
[9] M. Cunha, S. Paolinelli, J. Magn. Magn. Mater. 320 (2008) 2485–2489, https://doi.org/10.1016/j.jmmm.2008.04.054.
[10] M. Cunha, S. Paolinelli, Mater. Sci. Forum 467–470 (2004) 869–874, https://doi.org/10.4028/www.scientific.net/MSF.467-470.869.
[11] K. Lee, M. Huh, H. Lee, J. Park, J. Kim, E. Shin, O. Engler, J. Magn. Magn. Mater. 396 (2015) 53–64, https://doi.org/10.1016/j.jmmm.2015.08.010.
[12] F. Bachmann, R. Hielscher, H. Schaeben, Texture and Anisotropy of Polycrystals III, Solid State Phenom. vol. 160, Trans Tech Publications, 2010, pp. 63–68, , https://doi.org/10.4028/www.scientific.net/SSP.160.63.
[13] F.J.G. Landgraf, J.R.F. da Silveira, D. Rodrigues-Jr, J. Magn. Magn. Mater. 323 (2011) 2335–2339.
[14] J. Barros, J. Schneider, K. Verbeken, Y. Houbaert, J. Magn. Magn. Mater. 320 (2008) 2490–2493.
[15] G. Bertotti, IEEE Trans. Magn. 24 (1988) 621–630, https://doi.org/10.1109/20.43994.
[16] F.J.G. Landgraf, M. Emura, J.C. Teixeira, M.F. de Campos, J. Magn. Magn. Mater. 215–216 (2000) 97–99, https://doi.org/10.1016/S0304-8853(00)00076-7.
[17] M.F. de Campos, J.C. Teixeira, F.J.G. Landgraf, J. Magn. Magn. Mater. 301 (2006) 94–99, https://doi.org/10.1016/j.jmmm.2005.06.014.
[18] M.F. de Campos, T. Yonamine, M. Fukuhara, F.J.G. Landgraf, C.A. Achete, F.P. Missell, IEEE Trans. Magn. 42 (2006) 2812–2814, https://doi.org/10.1109/TMAG.2006.879897.
[19] G. Ban, P.E.D. Nunzio, S. Cicale, T. Belgrand, IEEE Trans. Magn. 34 (1998) 1174–1176, https://doi.org/10.1109/20.706438.
[20] C.-K. Hou, J. Magn. Magn. Mater. 162 (1996) 280–290, https://doi.org/10.1016/S0304-8853(96)00268-5.
[21] L. Toth, J. Jonas, D. Daniel, R. Ray, Metall. Trans. A-Phys. Metall. Mater. Sci. 21 (1990) 2985–3000, https://doi.org/10.1007/BF02647219.